HHS Public Access

Author manuscript

Alcohol Clin Exp Res. Author manuscript; available in PMC 2019 October 01.

Published in final edited form as:

Alcohol Clin Exp Res. 2018 October ; 42(10): 1883–1896. doi:10.1111/acer.13854.

Lower prefrontal and hippocampal volume and Diffusion Tensor Imaging differences reflect structural and functional abnormalities in abstinent individuals with Alcohol Use Disorder

Ashwini Kumar Pandey, Ph.D.[#a,*], **Babak Assai Ardekani, Ph.D.**[#b], **Chella Kamarajan, Ph.D.**[a], **Jian Zhang, Ph.D.**[a], **David Balin Chorlian, MS**[a], **Kelly Nicole-Helen Byrne, MS**[b], **Gayathri Pandey, Ph.D.**[a], **Jacquelyn Leigh Meyers, Ph.D.**[a], **Sivan Kinreich, Ph.D.**[a], **Arthur Stimus, MBA**[a], and **Bernice Porjesz, Ph.D.**[a]

[a]Henri Begleiter Neurodynamics Laboratory, SUNY Downstate Medical Center, Brooklyn, NY 11203, USA.

[b]The Nathan S. Kline Institute for Psychiatric Research, Orangeburg, NY 10962, USA.

[#] These authors contributed equally to this work.

Abstract

Background: *Alcohol use disorder* (AUD) is known to have adverse effects on brain structure and function. Multimodal assessments investigating volumetric, diffusion, and cognitive characteristics may facilitate understanding of the consequences of long-term alcohol use on brain circuitry, their structural impairment patterns, and their impact on cognitive function in AUD.

Methods: *voxel-and surface-based volumetric estimations*, *diffusion tensor imaging* (DTI), and neuropsychological tests were performed on 60 individuals: 30 abstinent individuals with AUD (DSM-IV) and 30 healthy controls. Group differences in the volumes of cortical and subcortical regions, *fractional anisotropy* (FA), *axial, and radial diffusivities* (AD and RD), and performance on neuropsychological tests were analyzed and the relationship among significantly different measures were assessed using canonical correlation.

Results: AUD participants had significantly smaller volumes in left pars orbitalis, right medial orbitofrontal, right caudal middle frontal, and bilateral hippocampal regions, lower FA in nine *white matter* (WM) regions, and higher FA in left thalamus, compared to controls. In AUD, lower FA in six out of nine WM regions were due to higher RD and due to lower AD in the left external capsule. AUD participants scored lower on problem-solving ability, visuospatial memory span, and working memory. Positive correlations of prefrontal cortical, left hippocampal volumes, and FA in four WM regions with visuospatial memory performance and negative correlation with

[*]Address for reprints and correspondence: Ashwini Kumar Pandey, Ph.D., Henri Begleiter Neurodynamics Laboratory, Department of Psychiatry and Behavioral Sciences, 450 Clarkson Avenue, MSC #1203, Brooklyn, NY 11203, USA., Ashwini.Pandey@downstate.edu, Tel: 1-718-270-2913, Fax: 1-718-270-4081.

Contributors

Conceptualization and design of the study: BP, BAA, AKP, CK. MRI recordings: BAA, KNHB. Neuropsychological tests: AKP, CK, AS, DBC. Data analyses: AKP, BAA, JZ, DBC, SK. Manuscript writing: AKP, BAA, BP, CK. Corrections/review/suggestions: BP, BAA, CK, KNHB, JZ, AS, DBC, GP, JLM, SK.

Conflict of interest

All of the coauthors reported no financial interests or potential conflicts of interest.

lower problem-solving ability were observed. Significant positive correlation between age and FA was observed in bilateral putamen.

Conclusions: Findings showed specific structural brain abnormalities to be associated with visuospatial memory and problem-solving ability related impairments observed in AUD. Higher RD in six WM regions suggests demyelination and lower AD in left external capsule suggests axonal loss in AUD. The positive correlation between FA and age in bilateral putamen may reflect accumulation of iron depositions with increasing age.

Keywords

DTI; hippocampal volume; fractional anisotropy; axial and radial diffusivity; neuropsychological tasks

1. Introduction

Alcohol use disorder (AUD) is reported to have adverse effects on brain structure and function (Squeglia et al., 2014a, Zahr and Pfefferbaum, 2017, Zahr et al., 2017). Compared to various clinical syndromes associated with alcohol use, gross brain pathology is generally absent in uncomplicated AUD (Zahr and Pfefferbaum, 2017). However, the effects of long-term alcohol use on the brain in those with uncomplicated AUD may manifest in subtle structural abnormalities that persist following abstinence from alcohol, potentially contributing to mild to moderate impairment of higher-order cognitive functioning characterized as memory, executive function, visuospatial ability, and social cognitive deficits (Easton et al., 2008, Ferrett et al., 2010, Johansen-Berg, 2010, Kopera et al., 2012, Le Berre et al., 2017, Sullivan et al., 2010). However, expected correlations between simple measures such as brain volumes and performance on relevant neuropsychological tests in AUD have not always been observed (Zahr et al., 2017). Instead, fronto-fugal circuits, including frontocerebellar, frontolimbic, and frontostriatal networks affected by AUD, have been proposed to underlie some of the distinct cognitive and motor function impairments observed in AUD (Sullivan and Pfefferbaum, 2005, Thiebaut de Schotten et al., 2015). Generally, bivariate correlations have been used to examine the association of either volume or diffusion characteristics with performance on neuropsychological tests in AUD (e.g., Colrain et al., 2011, Pitel et al., 2012a). However, often ignored is the association of impairments in circuit-related systems with cognitive and motor impairments. For example, several studies on long-term alcohol use/exposure using structural *magnetic resonance imaging* (MRI) and *diffusion tensor imaging* (DTI) have shown reduced volume in cortical and subcortical *gray matter* (GM) regions (De Bellis et al., 2000, Kroenke et al., 2014, Treit et al., 2013, Zahr and Pfefferbaum, 2017), and *white matter* (WM) microstructural tissue abnormalities (Bagga et al., 2014, Monnig et al., 2013, Thayer et al., 2013, Zahr and Pfefferbaum, 2017, Zorlu et al., 2014), suggesting their role in cognitive impairments. However, few studies have investigated the relationship of volumetric and/or diffusion characteristics with performance on neuropsychological tests (e.g., Chanraud et al., 2009, Schulte et al., 2012). Combining multimodal assessments such as volumetric and diffusion characteristics can further the understanding of their relationship with performance on

neuropsychological tests to accurately characterize structural and functional abnormalities in AUD.

Research has traditionally employed *voxel-based morphometry* (VBM) to estimate GM, WM, and cerebrospinal fluid (CSF) volumes on the voxel (millimeter) scale, whereas several scalar invariants derived from DTI, such as *fractional anisotropy* (FA) and *mean diffusivity* (MD), have been used to characterize WM microarchitecture (Alcauter et al., 2011, Belke et al., 2015, Kim et al., 2015). Reduction in GM volume in mature adults often reflects hypotrophy due to cellular loss and may be responsible for associated behavioral impairments (De Bellis et al., 2000, Kroenke et al., 2014, Treit et al., 2013) whereas lower FA is often interpreted as lower integrity of the WM, which may reflect factors including axonal count and density, degree of myelination, and fiber organization (Alcauter et al., 2011, Belke et al., 2015, Kim et al., 2015, Steinbrink et al., 2008). Recent studies have also reported changes in DTI characteristics of cortical and subcortical GM regions, pointing to various structural and physiological mechanisms to explain the findings (Camara et al., 2007, Chanraud et al., 2009, Douaud et al., 2009, Hasan et al., 2009, Lebel et al., 2008, Pfefferbaum et al., 2010a, Wang et al., 2010a, Zhan et al., 2012, Zhao et al., 2012). The utility of DTI analysis in both WM and GM is becoming increasingly evident with animal models, shedding light on the microarchitecture of the WM, where lower *axial diffusivity* (AD) is interpreted as a specific marker of axonal damage, loss, and density (Harsan et al., 2006, Sun et al., 2006) and higher *radial diffusivity* (RD) as a marker of dysmyelination and demyelination (Concha et al., 2010, Harsan et al., 2006, Mills and Tamnes, 2014, Tyszka et al., 2006), and as evidence of various physiological processes and changes in the GM. Therefore, analysis of multiple DTI measures, such as AD and RD together with FA, may aid in interpreting WM and GM findings. For example, examining the relative contribution of higher RD that suggests demyelination and lower AD that suggests lower axonal density would more specifically explain lower WM integrity (Alexander et al., 2007) and possibly their relative impact on brain function.

The present study investigates differences in brain volume, DTI (i.e., FA, AD, and RD), and performance on neuropsychological tests among abstinent individuals with AUD (DSM-IV) relative to controls. The study also examines the association of these structural brain abnormalities with performance deficits on neuropsychological tests of planning and problem-solving ability, visuospatial memory span, and working memory. Based on previous research, we hypothesized that abstinent individuals with AUD would have smaller volumes in prefrontal cortical regions, hippocampal regions, basal ganglia regions, infratentorial and cerebellar regions, and lower microstructural integrity in WM regions, and that these abnormalities would be associated with poorer performance on neuropsychological tasks

2. Materials and Methods

2.1. Participants

The sample comprised sixty individuals that included thirty abstinent male participants with AUD (DSM-IV criteria) [M_{age}(SD)=41.42(7.31) years] and thirty healthy male controls [M_{age}(SD)=27.44(4.74) years]. Controls were recruited through advertisements and screened to exclude any personal and/or family history of major medical, psychiatric, or substance-

related disorders. The participants with AUD were recruited from alcoholism treatment centers in and around NYC after they had been detoxified and not in withdrawal. None of the participants with AUD met DSM-IV criteria for substance use disorders. (see Table 1).

A modified version of the *semi-structured assessment of genetics of alcoholism* (SSAGA; Bucholz et al., 1994) was administered to assess alcohol/substance use and related disorders and family history of these disorders. Individuals with moderate and severe cognitive deficits (<21) on the *mini-mental state examination* (Folstein et al., 1975) were excluded from the study. Participants were instructed to abstain from alcohol and other substances for at least five days prior to the neuroimaging and neuropsychological assessments and were screened on the day of testing. Individuals who tested positive on the alcohol breathalyzer test or reported substance use were either rescheduled or excluded from the study. Individuals with hearing/visual impairment, liver disease, or history of head injury were also excluded. Standard protocols of recruitment for MRI were followed to ensure participants' safety during the scan. Informed consent was obtained from all participants. Experimental procedures and human research protection plans were carried out in accordance with the Declaration of Helsinki and were approved by the Institutional Review Boards.

2.2. Image acquisition, processing, and analysis

For full details of image acquisition, processing, and analysis, see supplementary material. Briefly, imaging was performed using a 3.0 Tesla Siemens Tim Trio MRI (Erlangen, Germany). A high-resolution three-dimensional T1-weighted *magnetization-prepared rapid gradient-echo* (MPRAGE) image with TR=2500 ms, TE=3.5 ms, TI=1200 ms, flip angle=8°, matrix size=256×256×192, and voxel size=1×1×1 mm^3; and a *turbo spin-echo* (TSE) *proton-density* (PD)-weighted image with TR=7000 ms, TE=11 ms, TI=1200 ms, matrix size=256×256×72, and voxel size=1×1×2 mm^3 were acquired. DTI included a double spin-echo *echo-planar imaging* (EPI) sequence with 37 measurements, 7 at b=0 and 30 at b=1000 s/mm^2 with uniformly distributed diffusion-sensitizing gradient directions, TR=9000 ms, TE=91 ms, matrix size=128×128×72, and voxel size=2×2×2 mm^3.

Diffusion tensors (D) were estimated and FA, MD, AD, and RD maps were calculated based on the estimated tensors in the native space. Group differences in the standardized FA maps were computed using voxelwise two-tailed t-tests with a voxelwise $p<0.01$ and the cluster size method (Forman et al., 1995) of correction for multiple comparisons. Fifteen FA clusters were found to be significantly different between AUD and control groups. Average FA, AD, and RD values in these clusters were extracted for further ROIs-neuropsychological analyses.

T1-weighted MPRAGE scans were parcellated and segmented into anatomical regions using *recon-all* program of the FreeSurfer (version 6.0; The General Hospital Corporation, Boston, MA). Image analysis in FreeSurfer has been previously described (Fischl and Dale, 2000). Briefly, after basic preprocessing, the white matter and pial surfaces were identified by creating a mesh around the white matter and pial voxels. Surface-based maps of each individual scan were constructed using a manually labeled training dataset (Desikan et al., 2006). The anatomical accuracy of FreeSurfer's automated parcellations and segmentations were visually inspected. Finally, volumetric measurements for each cortical and subcortical

region were obtained through automated calculation of the distances between their surface and white matter border using *recon-all* program.

In addition, we used a multi-atlas hippocampus segmentation algorithm (Heckemann et al., 2006) implemented in-house to measure *hippocampal volume* (HV) for cross-validation purposes. The automated hippocampus segmentations on all 60 participants were visually inspected for accuracy using the *ITK-SNAP* (www.itksnap.org) software (Yushkevich et al., 2006). An example of the automatically segmented hippocampus displayed using *ITK-SNAP is* shown in Figure 1a in the results section. Quantitative accuracy assessments using leave-one-out cross-validation yielded an average Dice index of 0.86 between manual and automatic segmentations.

2.3. Neuropsychological task measures

Computerized versions of the *Tower of London test* (TOLT) and the *visual span test* (VST) were administered using the *Colorado assessment tests* for cognitive and neuropsychological assessment (Davis and Keller, 2002).

The TOLT was used to assess planning and problem-solving ability (Shallice, 1982). On a computer screen, participants were shown a window on the left (working area) and a window on the right (goal position) with prearranged color beads placed on pegs. They were instructed to move the colored beads one-by-one in the working area until the arrangement on the goal position is achieved in as few moves as possible. The test consisted 21 trials with 3, 4, and 5 colored beads placed on respective number of pegs, comprising 7 problems per puzzle-type. Besides the total, separately for each puzzle-type, five performance measures were analyzed: *excess moves-made* (EM), *pickup-time*, *think-time*, *total trials-time*, and *average trial-time*.

The VST was used to assess visuospatial memory span and working memory with both forward and backward span tests included. Participants were shown eight boxes on a computer screen that illuminated in a designated sequence. Two trials for each 2–8 illuminated box sequences were presented that either were required to be repeated as seen (i.e., forward) or in reverse order (i.e., backward). The length of a sequence increased by one on a correct recall. The task ended upon incorrect recalls on both trials of the same sequence-length or correctly recalled all 8 sequence-lengths. Four performance measures: *total correct* (TC), *maximum sequence-length achieved* (Span), *total average time*, and *total correct-average time* for each of the *forward* (F) and *backward* (B) conditions were analyzed.

2.4. Statistical analyses

Student's *t*-tests were computed to determine group differences in age, education, and alcohol/substance use variables (Table 1). Linear model (LM) fits were performed to determine group differences for the cortical and subcortical region volumetric estimates, and the FA, AD, RD values in the 15 clusters identified in the voxelwise analysis of the DTI maps. Intracranial volume (ICV) used as covariates for the volumes of cortical and subcortical regions whereas only age was used as a covariate for all DTI measures. To determine the correct *p*-value threshold for a *familywise error rate* (FWER) of 5% for all

group comparisons, permutation tests (10,000 iterations) of all the LMs were performed to determine the expected FWER when the hypothesis of no group difference was true. The *p*-value for a single comparison was selected to guarantee that the FWER (type I error α) was controlled at < 0.05 level. Paired *t*-test was computed to determine group-independent difference between bilateral putamen. Partial correlation was performed to analyze the relationship between bilateral HV while controlling for age and ICV. To analyze the relationship between length of abstinence and volumetric, diffusion, and neuropsychological measures in the AUD group, partial correlations were performed while controlling for age and ICV and significance levels were checked using a Bonferroni *correction for multiple testing* (CMT).

LM and generalized linear models (GLM) were used to analyze the neuropsychological performance data with age as a covariate. Log transformations were applied to time measures and analyzed using LM assuming a normal distribution and identity link function. Integer-valued variables (e.g., EM) were analyzed using zero-inflated count models combining a point mass at zero with a negative binomial distribution model to reflect the over-dispersion of the data with a log-link function using GLM. For the VST measures (e.g., Span), cumulative logit models (Agresti, 2012) were applied. The log-likelihood test was used to compare the models, and goodness of fit test was used to select the most parsimonious model.

Canonical correlations were computed to determine associations between sets of volumetric and DTI measures with the set of neuropsychological performance measures. Only those variables that were significantly different between groups formed the respective sets (see Table 2 and Figures 2 and 5 in the results section). The top significant canonical correlations were selected for further examination.

3. Results

AUD participants were significantly older [$t(49.71)=8.78$, $p<0.0001$], had fewer years of education [$t(58)=-7.00$, $p<0.0001$], earlier age of onset of regular alcohol use [$t(40)=-4.67$, $p<0.0001$], higher quantity [$t(34.57)=5.58$, $p<0.0001$] and frequency [$t(39.18)=7.97$, $p<0.0001$] of alcohol use during heavy use period, longer length of abstinence [$t(31.97)=3.89$, $p<0.0005$], higher quantity of tobacco use [$t(24)=5.19$, $p<0.0001$], and higher frequency of marijuana use [$t(11.74)=2.50$, $p<0.03$]. However, the groups did not differ in the quantity of occasional alcohol use and frequency of alcohol and tobacco use during the last six months before participating in the study. Positive correlations between length of abstinence and volumes of bilateral caudate, pallidum, cerebral WM, mid posterior corpus callosum, and total subcortical GM were found, but none of them survived CMT, hence were not reported. Group differences (AUD vs. controls) were evaluated against FWER ($\alpha<0.05$) based on permutation test-based CMT. Based on FWER, cortical volume measures with $p<0.0022$ and subcortical volume measures with $p<0.0088$ were considered significant. Compared to controls, AUD participants had significantly smaller volume in left parsorbitalis [$F=10.73$, $p<0.002$], right medial orbitofrontal [$F=10.57$, $p<0.002$], right caudal middle frontal cortices [$F=16.60$, $p<0.0002$], and significantly smaller left [$F=7.74$, $p<0.007$] and right HV [$F=8.16$, $p<0.006$]. Left and right HV had within subject significant

correlation (r=0.709, p=4.82×10−^{10}) after controlling for age and ICV. Figures 1b and 2 illustrate the significant volumetric differences between the groups.

Figure 3 illustrates axial sections through the brain with crosshairs on the peak statistic MNI coordinates of the 15 FA clusters with significant group differences in voxelwise analysis. These clusters were labeled as GM01–03 if located in gray matter regions and WM01–12 if located in white matter regions.

Table 2 and Figure 5 illustrate group differences in FA, AD, and RD after controlling for age. Clusters are sorted, labeled, and presented based on whether they were located in GM or WM. The GM regions are shown in the gray and WM regions in the white backgrounds in Figure 5. Positive valence on the scale in the difference plots in Figure 5 indicates higher values, and negative valence indicates lower values in the AUD group relative to controls.

Similar to volumetric difference analysis, based on FWER (α<0.05), FA and AD differences with p<0.0068, and RD differences with p<0.0064 were considered significant. Group differences in left and right (GM01/02) putamen, right superior longitudinal fasciculus (WM06), callosal body (WM07), and left superior corona radiata (WM10) were rendered nonsignificant after controlling for age (Table 2). Significant positive correlations between age and bilateral putamen (Left: R^2=0.518; Right: R^2=0.531), with a group-independent greater left than right asymmetry in the putamen FA [paired t(59)=10.04, p<0.0001], were also observed (Figure 4). In remaining 10 clusters, AUD participants had significantly lower FA in WM compared to controls, except in left thalamus (GM03) where the FA was higher in the AUD group (Table 2).

Analysis of AD and RD revealed that after controlling for age, lower FA values in left external capsule (WM02), left superior longitudinal fasciculus (WM05), left splenium of corpus callosum (WM08), left anterior corona radiata (WM09), right superior corona radiata (WM11), and left occipital white matter (WM12) clusters in the AUD group were due to higher average RD whereas lower FA in left external capsule (WM03) was due to lower average AD (Table 2; Figure 5).

AUD participants made more moves (EM_3B) than required to complete 3 pegs/beads puzzle-type problems on the TOLT and scored lower on correct trial-count of visuospatial memory span (TC_F), memory span (Span_F), and working memory (Span_B) on the VST compared to controls (Table 3).

Full models including AD and RD as predictors for the performance on neuropsychological tests as criterion measures were found to be nonsignificant in canonical analyses. The analysis of the 5 volumetric measures (set-1) as predictors of the 4 neuropsychological task performances (set-2) yielded four dimensions with standardized canonical correlation coefficients (R_c) of 0.57, 0.45, 0.34, and 0.17, respectively. The full model was statistically significant [Wilks's λ=0.46 criterion, F(20,170.10)=2.25, p<0.003] and explained about 54% of the variance shared between variable sets. Given the squared canonical correlation coefficients (R_c^2) effects for each dimension (0.33, 0.21, 0.12, and 0.03), only *Dimension one* was considered noteworthy in the context of this study (33% of shared variance). The structure coefficients (R_s) showed that all four neuropsychological performance scores

contributed to the synthetic criterion variable (set-2) whereas left HV, left parsorbitalis volume (LParsOrbV), right medial orbitofrontal volume (RMeOFV), and right caudal middle frontal volume (RCMiFV) were the main contributors to the predictor synthetic variable (set-1). The respective squared structure coefficients (R_s^2) for both criterion and predictor variables supported these conclusions and are highlighted in bold (Table 4). The R_s of visuospatial memory performance scores were positively related to each other and negatively related to lower problem-solving ability (EM_3B) in the criterion variable (set-2). Interestingly, as the R_s of volumetric measures in the predictor variable (set-1) were positively related to each other, they were also positively related to visuospatial memory performance and negatively related to lower problem-solving ability in the criterion variable (set-2).

The analysis of the 10 FA measures (set-1) as predictors of the 4 neuropsychological task performances (set-2) as criterion measures yielded four dimensions with R_c of 0.72, 0.43, 0.37, and 0.17, respectively. The full model was statistically significant [Wilks's λ=0.32 criterion, $F(40,176.28)=1.53$, $p<0.034$] and explained about 68% of the variance shared between the variable sets. Given the R_c^2 effects for each dimension (0.52, 0.19, 0.14, and 0.03), only *Dimension one* was considered noteworthy in the context of this study (52% of shared variance). The R_s showed that all four neuropsychological performance scores contributed to the synthetic criterion variable (set-2), whereas FA in left thalamus (GM03), left frontal white matter (WM01), left superior longitudinal fasciculus, (WM05), left splenium of corpus callosum (WM08), and left anterior corona radiata (WM09) were main contributors to the predictor synthetic variable (set-1). The respective R_s^2 for both criterion and predictor variables supported these conclusions and are highlighted in bold (Table 5). The R_s of visuospatial memory performance scores were positively related to each other and negatively related to lower problem-solving ability. Interestingly, as the R_s of FA measures from WM regions (set-1) were positively related to each other and negatively related to left thalamus, they were also positively related to visuospatial memory performance and negatively related to lower problem-solving ability (set-2). Conversely, signs on FA in left thalamus (set-1) and criterion variables (set-2) indicate that FA in left thalamus was positively related to lower problem-solving ability and negatively related to visuospatial memory performance.

4. Discussion

The present study utilized multi-modal neuroimaging to examine both volumetric and diffusion data and their relation to neuropsychological task performance. Importantly, we found that compared to the control group, the AUD group had: 1) lower problem-solving ability, visuospatial memory span, and working memory; 2) smaller volumes in left parsorbitalis, right medial orbitofrontal, right caudal middle frontal regions, and bilateral hippocampi; and 3) lower FA in multiple WM regions and higher FA in the left thalamus. The lower FA values in 6 WM regions were due to higher RD in the AUD group, except the left external capsule (WM03) where FA was explained by lower AD. 4) The FA in bilateral putamen was significantly and positively associated with age, which explained the group differences observed in voxelwise analysis. 5) Canonical dimension explained shared variance among prefrontal and hippocampal volumes, FA values, and neuropsychological

task performance. The prefrontal cortical and left hippocampal volumes and FA in WM regions were positively related to visuospatial memory performance and negatively related to lower problem-solving ability. Conversely, FA in the left thalamus was negatively related to visuospatial memory performance and positively related to lower problem-solving ability.

4.1. Anatomical volumes

Consistent with previous reports, AUD participants had smaller volumes compared to controls in left parsorbitalis, right medial orbitofrontal, right caudal middle frontal cortical regions, and bilateral hippocampi (see for a review Zahr and Pfefferbaum, 2017). A recent study by Pfefferbaum et al. (2018) reported significantly steeper reduction of caudal middle frontal, superior frontal, and posterior cingulate cortical regions in heavy-drinking adolescents. Many of the same cortical regions were implicated in both studies, albeit failed surviving a CMT. For example, the superior frontal cortical region reported as significantly affected in the Pfefferbaum et al. (2018) study did not survive a CMT in the present study. Differing methodology (e.g., permutation tests vs. FDR), study design, and sample characteristics (e.g., adolescents vs. adult) likely contributed to these differences. Nevertheless, several findings, including that of caudal middle frontal cortical region, tended to be consistent across studies. Early age of regular drinking onset in the AUD group compared to controls in the present study (Table 1) also supports the conclusion of alcohol use in adolescents affecting cortical volume in these regions in the Pfefferbaum et al. (2018) study. Orbitofrontal cortical volume is reportedly affected by *Wernicke's Korsakoff Syndrome* (WKS) and the propensity to relapse following abstinence and older age are reported to be related to pronounced orbitofrontal atrophy in uncomplicated AUD (Beck et al., 2012, Durazzo et al., 2011, Zou et al., 2018).

HV deficits milder than that of WKS have been observed in uncomplicated AUD compared to healthy controls (Pitel et al., 2012b), which are attributed to loss of WM and decreased axonal diameter (Harding et al., 1997), glial cell loss (Korbo, 1999), or reduced incorporation of newly formed neurons to the dentate gyrus (He et al., 2005). The hippocampus plays a central role in the formation, consolidation, and retention of recent (or declarative) memories (Burgess et al., 2002, Tamnes et al., 2014). Memory impairments have been observed in early abstinent AUD individuals (e.g., Kopera et al., 2012) and various mechanisms implicating hippocampus have been proposed (Chanraud et al., 2009, Zahr et al., 2017). Therefore, these results also provide a neuroanatomical substrate for memory impairments in AUD.

However, no significant differences either in basal ganglia nodes of reward circuitry (i.e., caudate, putamen, amygdala, and nucleus accumbens) or in total infratentorial volume, pons, and cerebellum were observed as previously reported (Sullivan et al., 2005, Zahr and Pfefferbaum, 2017). The different methodological and sample characteristics may be contributing to the differences in results. In contrast to more recently abstinent AUD samples used in previous studies, the majority of AUD participants (22/30) in the present study were long-term abstinent and few (8/30) were abstinent for less than six months. *Post hoc* partial correlations yielded significant positive correlations between abstinence-length and volumes of bilateral caudate, pallidum, cerebral WM, mid posterior corpus callosum, and total

subcortical GM, suggesting association of volumes in these regions with abstinence-length, similar to previous findings (Zahr and Pfefferbaum, 2017). However, associations did not survive a CMT. Despite reports of recovery of brain volumes with abstinence, mechanisms of recovery and effects of abstinence-length remain unclear due to factors such as aging (Zahr and Pfefferbaum, 2017). Future studies should investigate recovery of brain volume combining cross-sectional and longitudinal data while controlling for age and abstinence-length, to better understand the extent of recovery in AUD following abstinence.

Lower prefrontal cortical volume in AUD may be implicated in the observed poorer performance on neuropsychological tests and cognitive functions involving these regions (De Rosa et al., 2004, Fassbender et al., 2004). However, it has also been suggested that executive function and frontal lobe volume deficits were associated in at-risk (Family history of AUD) individuals, while spatial and memory related deficits and temporoparietal volume deficits were associated as a consequence of alcohol use (Squeglia et al., 2014a, Squeglia et al., 2014b). Therefore, the differential effects of familial risk and heavy alcohol use on the prefrontal cortical volume must be accounted for to examine potential cause/s of smaller prefrontal cortical volume in AUD.

4.2. Diffusion Tensor Imaging measures

DTI analysis identified 9 WM regions including frontal white matter, external capsule, superior longitudinal fasciculus, splenium of corpus callosum, anterior corona radiate, and occipital white matter of the left hemisphere and right superior corona radiata where AUD participants had lower FA compared to controls (Table 2, Figure 5), suggesting lower WM integrity confirming previous findings (Bagga et al., 2014, Fortier et al., 2014, Monnig et al., 2013, Pfefferbaum et al., 2010b). The callosal body was also found to be affected (unadjusted $p<0.008$) as commonly reported (e.g., Pitel et al., 2010) but did not survive a CMT. These FA differences were further explained by the contribution of higher RD in 6 WM regions and lower AD in left external capsule (WM03). Proton diffusion in tissue is highly sensitive to differences in the microstructural architecture of cellular membranes. Larger average spacing between membrane layers will result in higher diffusivity, whereas smaller spaces will lead to lower diffusivities (Alexander et al., 2007). Research has demonstrated that the parallel organization of WM fiber bundles and axonal membranes is the primary determinant of diffusion anisotropy in both peripheral nerves and the central nervous system WM, while myelin integrity appears to modulate the degree of anisotropy (Beaulieu, 2002, Concha et al., 2010). For example, rodent dysmyelination models showed that FA values still indicate anisotropy and reduce only by ~15% in the complete absence of myelin (cited from Mills and Tamnes, 2014). Almost all studies of myelination with normal brain development (Neil et al., 1998) or demyelination with disease-related processes (Sun et al., 2006) have found less diffusion anisotropy, where axons are less myelinated. Studies of dysmyelination and demyelination have also confirmed increased RD i.e., diffusion away from the axis (Harsan et al., 2006, Song et al., 2005, Tyszka et al., 2006), whereas AD, i.e., diffusion along the axis, has been suggested to be a more specific marker of axonal damage, loss, and density (Harsan et al., 2006). Precise mechanisms aside, AD and RD provide more specific information about tissue diffusion properties than FA alone.

Therefore, the current findings of higher RD in the 6 WM regions and lower AD in left external capsule (WM03) of AUD participants (Table 2, Figure 5) suggest that lower WM integrity may be interpreted as a result of demyelination in six regions. Lower WM in the left external capsule (WM03) may also be explained as a result of lower axonal density or its loss. Zorlu et al. (2014) reported higher AD and RD values but no differences in FA between AUD and control groups, indicating that these metrics provide additional information. Lower WM integrity may also suggest relatively lower levels of brain activation during cognitive processing due to tardy signal processing in the brains of individuals with AUD that perhaps reflects in their subpar performance on various cognitive and behavioral tasks. Accordingly, there is ample evidence showing relatively lower overall task-related cortical activation (for a review see Pandey et al., 2012a), longer reaction-time (Pandey et al., 2015, Pandey et al., 2012b, Smith et al., 2014), and longer event-related potential (ERP) peak latencies (Porjesz et al., 1987, Schuckit et al., 1988, Smith et al., 2014) while performing cognitive and motor tasks, which are indicators of resource allocation for response strength and associated cortical processing speeds in individuals with AUD. Given that impulsive and premature response tendencies are characteristic of AUD, these frequently reported findings may seem counterintuitive. However, Lawrence et al. (2009) have suggested that impaired inhibitory control in alcoholism occurs in the context of psychomotor slowing. Future research involving longitudinal structural and functional aspects in AUD can specifically test these hypotheses.

Changes in Diffusion Tensor Imaging characteristics of cortical and subcortical GM regions have also been recently reported and various mechanisms involving structural and physiological characteristics have been proposed (Camara et al., 2007, Douaud et al., 2009, Hasan et al., 2009, Lebel et al., 2008, Pfefferbaum et al., 2010a, Wang et al., 2010a, Zhan et al., 2012, Zhao et al., 2012). Specific examples of increased anisotropy include, loss of myelinated fibers passing through GM structures (Douaud et al., 2009), targeted loss of certain dendritic connections (Hasan et al., 2008), and aging-related neural and dendritic elimination, (Hasan et al., 2009), tissue compaction and gliosis, (Wang et al., 2010b), and iron deposition (Pfefferbaum et al., 2010a). Rulseh et al. (2013) reported iron-dependent signal attenuation in vitro (resulting in increased FA) as well as an apparent FA increase and mean diffusivity decrease in vivo as signal attenuated in putamen and concluded that ferritin-bound iron makes an important contribution to DTI metrics in low-signal, isotropic, iron-rich regions. Specifically, it is likely that the apparent increase in FA with age in bilateral putamen may be due to an upward bias in the estimated diffusion anisotropy which is inversely proportional to the loss of MRI signal due to iron deposition. Although iron continues to accumulate throughout the lifespan in healthy cortical and subcortical GM, it occurs over a limited range beyond 30 years of age. Notably, the most gradual accumulation in the basal ganglia occurs in putamen (Rulseh et al., 2013). Therefore, evidence suggests that accumulation of iron deposits in bilateral putamen due to increasing age causes MRI signal attenuation reflected in the apparent increase in FA (Pfefferbaum et al., 2010a). Therefore, our finding of higher FA in bilateral putamen in the AUD group, attributed as an effect of age and not due to group membership or significant changes in AD or RD, tends to confirm this interpretation. We also found a significant lateral asymmetry in putamen apparent FA which, if replicated in independent studies, could indicate higher iron

concentration on the left. Additionally, we also found higher apparent FA in the left thalamus. Although the specific mechanism causing apparent increase in FA in the thalamus remains unclear, there are reports of unilateral temporary increase of FA in the thalamus contralateral to the affected body side during extremity pain episodes in MS (Deppe et al., 2013). Also, FA in thalamus is an independent predictor of *White Matter Hyperintensities* (WMH) accrual over a 4-year period in community dwelling older subjects (Cavallari et al., 2014). Research also suggests GM microstructure aberrations measured as *apparent diffusion coefficients* (ADC) in parahippocampal regions, frontal cortex, and left temporal cortex as responsible, at least partially, for episodic memory deficits in AUD (Chanraud et al., 2009). Therefore, considering volumetric shrinkage (Zahr and Pfefferbaum, 2017), microstructural aberrations and their relation to lower GM volume in AUD (Chanraud et al., 2009), the importance of thalamic structures for cognitive functions (see for a review Fama and Sullivan, 2015), and in light of aforementioned findings, it is important to report significant group and/or age modulated effects on FA of subcortical structures, including thalamus.

4.3. Neuropsychological task measures

Long-term alcohol use has been associated with mild to moderate cognitive impairments in memory and higher-order executive function, among others (Johansen-Berg, 2010, Kopera et al., 2012, Le Berre et al., 2017, Sullivan et al., 2010, Zahr et al., 2017). Current findings support these conclusions reporting lower problem-solving ability, lower visuospatial memory span, and working memory in AUD. Interestingly, AUD participants showed lower problem-solving ability only for the 3-pegs/beads puzzle-type in a task (TOLT) that also included puzzle-types with 4- and 5-pegs/beads. However, they did not show lower ability in preplanning or time spent in problem-solving. The 3 pegs/beads puzzle-type problems that require 3, 4, and 5 moves to solve tend to have a higher difficulty level compared to the 4- and 5-pegs/beads puzzle-types with similar move requirements (Dias and Seabra, 2012). Thus, AUD participants seem to display lower problem-solving ability only when the level of task-difficulty is higher. This suggests that cognitive deficits in AUD are subtle and manifest mainly in higher-order cognitive functions and/or in demanding circumstances.

4.4. Relationship between cortical and hippocampal volumes, Diffusion Tensor Imaging and cognitive measures

Our findings align with an expected relationship between structural and functional abnormalities. For example, significantly explained shared variances showed positive associations of left parsorbitalis, right medial orbitofrontal, right caudal middle frontal cortical volumes, left HV, FA in anteriorly situated frontal WM, superior longitudinal fasciculus, anterior corona radiata, and posteriorly situated left splenium of corpus callosum in the left hemisphere regions with performance on visuospatial memory span and working memory, and their (volumetric and FA measures) negative associations with lower problem-solving ability (Tables 4 and 5), suggesting the role of prefrontal focused circuitry in these cognitive functions. Conversely, FA in left thalamus had a negative association with visuospatial memory performance and a positive association with lower problem-solving ability (Table 5), suggesting that an increase in left thalamic FA may lead to cognitive impairments. Some of these results confirm previously reported volumetric and DTI

measures with functional association findings (Colrain et al., 2011, Pfefferbaum et al., 2000, Pitel et al., 2012a). Additionally, combined structural results and relative contributions of different GM and WM regions in explaining shared variance with performance on neuropsychological tests suggest abnormalities in brain circuits, rather than distinct brain regions, as responsible for the observed functional deficits. Zahr et al. (2017) have recently identified three independent and non-overlapping frontally-based networks (fronto-fugal), involving coordinated activities of several regions interacting with frontal structures rather than a single area in prefrontal cortices, that mediate specific neuropsychological deficits in AUD. These authors propose that abnormalities of brain structure and function are due to AUD and not merely aging. More refined knowledge of compromised and spared structures and functions in AUD would help in determining mediational effects that could enhance therapeutic efforts to redirect neural recruitment from the usual but disrupted paths and networks to functional alternatives, possibly through behavioral therapy (Zahr et al., 2017). Future studies should investigate the relationship of structural characteristics and connectivity with functional connectivity, combining data from different techniques such as diffusion tractography with functional connectivity measures, including resting-state and event-related functional networks, in order to understand the link between structural and functional abnormalities in AUD.

4.5. Limitations and future directions

Although we employed statistical control for the effect of age, given the crucial importance of age-related brain changes in AUD, it is important that future studies with larger samples and age-matched balanced designs account for these confounding factors and confirm the current findings. Similarly, owing to recent equivocal findings on the effect of level of education on brain structure and function after controlling for IQ at age eleven (e.g., Cox et al., 2016), the effect of level of education was not controlled to avoid possible model-fitting errors. However, appropriate measures of intelligence should also be used to control for its effects to confirm the current findings. Other substance use in individuals with AUD without meeting criteria for substance use disorder is often observed as part of their clinical profile, including in the present sample. While it was beyond the scope of the present study, future studies should also control for other substance use in large clinical samples, and/or in more controlled animal studies to confirm the current findings. Some of the interpretations made in the present study are speculative in nature, given that those hypotheses were not directly tested and have been inferred from associations and evidence reported in the literature (e.g., Harsan et al., 2006, Rulseh et al., 2013). Future longitudinal structural and functional studies can specifically test these conclusions by investigating additional measures and analyses. Future investigations would also benefit from an integrative approach, employing a variety of complementary technologies to analyze and understand the interconnectivity of structural, functional, and behavioral systems affected by AUD. For example, combining volumetric, DTI, and histological examination of GM and WM would be important to shed light on causes of changes and on the basis of anisotropy observed in different parts of the brain along with functional imaging measures in order to directly assess relationships between structural and functional abnormalities.

Supplementary Material

Refer to Web version on PubMed Central for supplementary material.

Acknowledgements

This study was supported by Grants # R01 AA005524 and R01 AA002686 from the National Institute on Alcohol Abuse and Alcoholism (NIAAA). We are grateful for the valuable technical assistance of Elaine Bermudez, Carlene Haynes, Joyce Alonzia, Chamion Thomas, Anthony Feliciano, and Alec Musial.

References

Agresti A (2012) Categorical data analysis Wiley, Hoboken, N.J.

Alcauter S, Barrios FA, Diaz R, Fernandez-Ruiz J (2011) Gray and white matter alterations in spinocerebellar ataxia type 7: an in vivo DTI and VBM study. Neuroimage 55:1–7. [PubMed: 21147232]

Alexander AL, Lee JE, Lazar M, Field AS (2007) Diffusion tensor imaging of the brain. Neurotherapeutics : the journal of the American Society for Experimental NeuroTherapeutics 4:316–329. [PubMed: 17599699]

Anderson D, Ardekani BA, Burdick KE, Robinson DG, John M, Malhotra AK, Szeszko PR (2013) Overlapping and distinct gray and white matter abnormalities in schizophrenia and bipolar I disorder. Bipolar Disord 15:680–693. [PubMed: 23796123]

Antonius D, Prudent V, Rebani Y, D'Angelo D, Ardekani BA, Malaspina D, Hoptman MJ (2011) White matter integrity and lack of insight in schizophrenia and schizoaffective disorder. Schizophr Res 128:76–82. [PubMed: 21429714]

Ardekani BA, Bachman AH, Helpern JA (2001) A quantitative comparison of motion detection algorithms in fMRI. Magn Reson Imaging 19:959–963. [PubMed: 11595367]

Ardekani BA, Braun M, Hutton BF, Kanno I, Iida H (1995) A fully automatic multimodality image registration algorithm. J Comput Assist Tomogr 19:615–623. [PubMed: 7622696]

Ardekani BA, Guckemus S, Bachman A, Hoptman MJ, Wojtaszek M, Nierenberg J (2005) Quantitative comparison of algorithms for inter-subject registration of 3D volumetric brain MRI scans. J Neurosci Methods 142:67–76. [PubMed: 15652618]

Ardekani BA, Tabesh A, Sevy S, Robinson DG, Bilder RM, Szeszko PR (2011) Diffusion tensor imaging reliably differentiates patients with schizophrenia from healthy volunteers. Hum Brain Mapp 32:1–9. [PubMed: 20205252]

Bagga D, Sharma A, Kumari A, Kaur P, Bhattacharya D, Garg ML, Khushu S, Singh N (2014) Decreased white matter integrity in fronto-occipital fasciculus bundles: relation to visual information processing in alcohol-dependent subjects. Alcohol 48:43–53. [PubMed: 24388377]

Beaulieu C (2002) The basis of anisotropic water diffusion in the nervous system - a technical review. NMR Biomed 15:435–455. [PubMed: 12489094]

Beck A, Wustenberg T, Genauck A, Wrase J, Schlagenhauf F, Smolka MN, Mann K, Heinz A (2012) Effect of brain structure, brain function, and brain connectivity on relapse in alcohol-dependent patients. Arch Gen Psychiatry 69:842–852. [PubMed: 22868938]

Belke M, Heverhagen JT, Keil B, Rosenow F, Oertel WH, Stiasny-Kolster K, Knake S, Menzler K (2015) DTI and VBM reveal white matter changes without associated gray matter changes in patients with idiopathic restless legs syndrome. Brain and behavior 5:e00327. [PubMed: 26442748]

Bucholz KK, Cadoret R, Cloninger CR, Dinwiddie SH, Hesselbrock VM, Nurnberger JI, Jr., Reich T, Schmidt I, Schuckit MA (1994) A new, semi-structured psychiatric interview for use in genetic linkage studies: a report on the reliability of the SSAGA. J Stud Alcohol 55:149–158. [PubMed: 8189735]

Burgess N, Maguire EA, O'Keefe J (2002) The human hippocampus and spatial and episodic memory. Neuron 35:625–641. [PubMed: 12194864]

Camara E, Bodammer N, Rodriguez-Fornells A, Tempelmann C (2007) Age-related water diffusion changes in human brain: a voxel-based approach. Neuroimage 34:1588–1599. [PubMed: 17188516]

Cavallari M, Moscufo N, Meier D, Skudlarski P, Pearlson GD, White WB, Wolfson L, Guttmann CR (2014) Thalamic fractional anisotropy predicts accrual of cerebral white matter damage in older subjects with small-vessel disease. J Cereb Blood Flow Metab 34:1321–1327. [PubMed: 24824915]

Chanraud S, Leroy C, Martelli C, Kostogianni N, Delain F, Aubin HJ, Reynaud M, Martinot JL (2009) Episodic memory in detoxified alcoholics: contribution of grey matter microstructure alteration. PLoS One 4:e6786. [PubMed: 19707568]

Colrain IM, Sullivan EV, Ford JM, Mathalon DH, McPherson SL, Roach BJ, Crowley KE, Pfefferbaum A (2011) Frontally mediated inhibitory processing and white matter microstructure: age and alcoholism effects. Psychopharmacology (Berl) 213:669–679. [PubMed: 21161189]

Concha L, Livy DJ, Beaulieu C, Wheatley BM, Gross DW (2010) In vivo diffusion tensor imaging and histopathology of the fimbria-fornix in temporal lobe epilepsy. J Neurosci 30:996–1002. [PubMed: 20089908]

Cox SR, Dickie DA, Ritchie SJ, Karama S, Pattie A, Royle NA, Corley J, Aribisala BS, Valdes Hernandez M, Munoz Maniega S, Starr JM, Bastin ME, Evans AC, Wardlaw JM, Deary IJ (2016) Associations between education and brain structure at age 73 years, adjusted for age 11 IQ. Neurology 87:1820–1826. [PubMed: 27664981]

Davis HP, and Keller F. (2002) Colorado Assessment Tests (CATs), Version 1.2, Colorado Springs, Colorado., in Series Colorado Assessment Tests (CATs), Version 1.2, Colorado Springs, Colorado.

De Bellis MD, Clark DB, Beers SR, Soloff PH, Boring AM, Hall J, Kersh A, Keshavan MS (2000) Hippocampal volume in adolescent-onset alcohol use disorders. Am J Psychiatry 157:737–744. [PubMed: 10784466]

De Rosa E, Desmond JE, Anderson AK, Pfefferbaum A, Sullivan EV (2004) The human basal forebrain integrates the old and the new. Neuron 41:825–837. [PubMed: 15003180]

Deppe M, Muller D, Kugel H, Ruck T, Wiendl H, Meuth SG (2013) DTI detects water diffusion abnormalities in the thalamus that correlate with an extremity pain episode in a patient with multiple sclerosis. Neuroimage Clin 2:258–262. [PubMed: 24179780]

Desikan RS, Segonne F, Fischl B, Quinn BT, Dickerson BC, Blacker D, Buckner RL, Dale AM, Maguire RP, Hyman BT, Albert MS, Killiany RJ (2006) An automated labeling system for subdividing the human cerebral cortex on MRI scans into gyral based regions of interest. Neuroimage 31:968–980. [PubMed: 16530430]

Dias NM, Seabra AG (2012) Executive demands of the Tower of London task in Brazilian teenagers. Psychology & Neuroscience 5:63–75.

Douaud G, Behrens TE, Poupon C, Cointepas Y, Jbabdi S, Gaura V, Golestani N, Krystkowiak P, Verny C, Damier P, Bachoud-Levi AC, Hantraye P, Remy P (2009) In vivo evidence for the selective subcortical degeneration in Huntington's disease. Neuroimage 46:958–966. [PubMed: 19332141]

Durazzo TC, Tosun D, Buckley S, Gazdzinski S, Mon A, Fryer SL, Meyerhoff DJ (2011) Cortical thickness, surface area, and volume of the brain reward system in alcohol dependence: relationships to relapse and extended abstinence. Alcohol Clin Exp Res 35:1187–1200. [PubMed: 21410483]

Easton CJ, Sacco KA, Neavins TM, Wupperman P, George TP (2008) Neurocognitive performance among alcohol dependent men with and without physical violence toward their partners: a preliminary report. Am J Drug Alcohol Abuse 34:29–37. [PubMed: 18161641]

Fama R, Sullivan EV (2015) Thalamic structures and associated cognitive functions: Relations with age and aging. Neurosci Biobehav Rev 54:29–37. [PubMed: 25862940]

Fassbender C, Murphy K, Foxe JJ, Wylie GR, Javitt DC, Robertson IH, Garavan H (2004) A topography of executive functions and their interactions revealed by functional magnetic resonance imaging. Brain Res Cogn Brain Res 20:132–143. [PubMed: 15183386]

Ferrett HL, Carey PD, Thomas KG, Tapert SF, Fein G (2010) Neuropsychological performance of South African treatment-naive adolescents with alcohol dependence. Drug Alcohol Depend 110:8–14. [PubMed: 20227839]

Fischl B, Dale AM (2000) Measuring the thickness of the human cerebral cortex from magnetic resonance images. Proc Natl Acad Sci U S A 97:11050–11055. [PubMed: 10984517]

Folstein MF, Folstein SE, McHugh PR (1975) "Mini-mental state". A practical method for grading the cognitive state of patients for the clinician. J Psychiatr Res 12:189–198. [PubMed: 1202204]

Forman SD, Cohen JD, Fitzgerald M, Eddy WF, Mintun MA, Noll DC (1995) Improved assessment of significant activation in functional magnetic resonance imaging (fMRI): use of a cluster-size threshold. Magn Reson Med 33:636–647. [PubMed: 7596267]

Fortier CB, Leritz EC, Salat DH, Lindemer E, Maksimovskiy AL, Shepel J, Williams V, Venne JR, Milberg WP, McGlinchey RE (2014) Widespread effects of alcohol on white matter microstructure. Alcohol Clin Exp Res 38:2925–2933. [PubMed: 25406797]

Harding AJ, Wong A, Svoboda M, Kril JJ, Halliday GM (1997) Chronic alcohol consumption does not cause hippocampal neuron loss in humans. Hippocampus 7:78–87. [PubMed: 9138671]

Harsan LA, Poulet P, Guignard B, Steibel J, Parizel N, de Sousa PL, Boehm N, Grucker D, Ghandour MS (2006) Brain dysmyelination and recovery assessment by noninvasive in vivo diffusion tensor magnetic resonance imaging. J Neurosci Res 83:392–402. [PubMed: 16397901]

Hasan KM, Halphen C, Boska MD, Narayana PA (2008) Diffusion tensor metrics, T2 relaxation, and volumetry of the naturally aging human caudate nuclei in healthy young and middle-aged adults: possible implications for the neurobiology of human brain aging and disease. Magn Reson Med 59:7–13. [PubMed: 18050345]

Hasan KM, Halphen C, Kamali A, Nelson FM, Wolinsky JS, Narayana PA (2009) Caudate nuclei volume, diffusion tensor metrics, and T(2) relaxation in healthy adults and relapsing-remitting multiple sclerosis patients: implications for understanding gray matter degeneration. J Magn Reson Imaging 29:70–77. [PubMed: 19097116]

He DY, McGough NN, Ravindranathan A, Jeanblanc J, Logrip ML, Phamluong K, Janak PH, Ron D (2005) Glial cell line-derived neurotrophic factor mediates the desirable actions of the anti-addiction drug ibogaine against alcohol consumption. J Neurosci 25:619–628. [PubMed: 15659598]

Heckemann RA, Hajnal JV, Aljabar P, Rueckert D, Hammers A (2006) Automatic anatomical brain MRI segmentation combining label propagation and decision fusion. Neuroimage 33:115–126. [PubMed: 16860573]

Holmes CJ, Hoge R, Collins L, Woods R, Toga AW, Evans AC (1998) Enhancement of MR images using registration for signal averaging. J Comput Assist Tomogr 22:324–333. [PubMed: 9530404]

Johansen-Berg H (2010) Behavioural relevance of variation in white matter microstructure. Curr Opin Neurol 23:351–358. [PubMed: 20581685]

Kim SG, Jung WH, Kim SN, Jang JH, Kwon JS (2015) Alterations of Gray and White Matter Networks in Patients with Obsessive-Compulsive Disorder: A Multimodal Fusion Analysis of Structural MRI and DTI Using mCCA+jICA. PLoS One 10:e0127118. [PubMed: 26038825]

Kopera M, Wojnar M, Brower K, Glass J, Nowosad I, Gmaj B, Szelenberger W (2012) Cognitive functions in abstinent alcohol-dependent patients. Alcohol 46:665–671. [PubMed: 22703992]

Korbo L (1999) Glial cell loss in the hippocampus of alcoholics. Alcohol Clin Exp Res 23:164–168. [PubMed: 10029219]

Kroenke CD, Rohlfing T, Park B, Sullivan EV, Pfefferbaum A, Grant KA (2014) Monkeys that voluntarily and chronically drink alcohol damage their brains: a longitudinal MRI study. Neuropsychopharmacology 39:823–830. [PubMed: 24077067]

Lawrence AJ, Luty J, Bogdan NA, Sahakian BJ, Clark L (2009) Impulsivity and response inhibition in alcohol dependence and problem gambling. Psychopharmacology (Berl) 207:163–172. [PubMed: 19727677]

Le Berre AP, Fama R, Sullivan EV (2017) Executive Functions, Memory, and Social Cognitive Deficits and Recovery in Chronic Alcoholism: A Critical Review to Inform Future Research. Alcohol Clin Exp Res 41:1432–1443. [PubMed: 28618018]

Lebel C, Walker L, Leemans A, Phillips L, Beaulieu C (2008) Microstructural maturation of the human brain from childhood to adulthood. Neuroimage 40:1044–1055. [PubMed: 18295509]

Mahon K, Burdick KE, Wu J, Ardekani BA, Szeszko PR (2012) Relationship between suicidality and impulsivity in bipolar I disorder: a diffusion tensor imaging study. Bipolar Disord 14:80–89. [PubMed: 22329475]

Mills KL, Tamnes CK (2014) Methods and considerations for longitudinal structural brain imaging analysis across development. Dev Cogn Neurosci 9:172–190. [PubMed: 24879112]

Monnig MA, Caprihan A, Yeo RA, Gasparovic C, Ruhl DA, Lysne P, Bogenschutz MP, Hutchison KE, Thoma RJ (2013) Diffusion tensor imaging of white matter networks in individuals with current and remitted alcohol use disorders and comorbid conditions. Psychol Addict Behav 27:455–465. [PubMed: 22352699]

Neil JJ, Shiran SI, McKinstry RC, Schefft GL, Snyder AZ, Almli CR, Akbudak E, Aronovitz JA, Miller JP, Lee BC, Conturo TE (1998) Normal brain in human newborns: apparent diffusion coefficient and diffusion anisotropy measured by using diffusion tensor MR imaging. Radiology 209:57–66. [PubMed: 9769812]

Pandey AK, Kamarajan C, Manz N, Chorlian DB, Stimus A, Porjesz B (2015) Delta, theta, and alpha event-related oscillations in alcoholics during go/NoGo task: Neurocognitive deficits in execution, inhibition, and attention processing. Prog Neuropsychopharmacol Biol Psychiatry

Pandey AK, Kamarajan C, Rangaswamy M, Porjesz B (2012a) Event-related oscillations in alcoholism research: A review. Journal of Addiction Research and Therapy S7

Pandey AK, Kamarajan C, Tang Y, Chorlian DB, Roopesh BN, Manz N, Stimus A, Rangaswamy M, Porjesz B (2012b) Neurocognitive deficits in male alcoholics: an ERP/sLORETA analysis of the N2 component in an equal probability Go/NoGo task. Biol Psychol 89:170–182. [PubMed: 22024409]

Pardoe HR, Kucharsky Hiess R, Kuzniecky R (2016) Motion and morphometry in clinical and nonclinical populations. Neuroimage 135:177–185. [PubMed: 27153982]

Pfefferbaum A, Adalsteinsson E, Rohlfing T, Sullivan EV (2010a) Diffusion tensor imaging of deep gray matter brain structures: effects of age and iron concentration. Neurobiol Aging 31:482–493. [PubMed: 18513834]

Pfefferbaum A, Kwon D, Brumback T, Thompson WK, Cummins K, Tapert SF, Brown SA, Colrain IM, Baker FC, Prouty D, De Bellis MD, Clark DB, Nagel BJ, Chu W, Park SH, Pohl KM, Sullivan EV (2018) Altered Brain Developmental Trajectories in Adolescents After Initiating Drinking. Am J Psychiatry 175:370–380. [PubMed: 29084454]

Pfefferbaum A, Rosenbloom MJ, Fama R, Sassoon SA, Sullivan EV (2010b) Transcallosal white matter degradation detected with quantitative fiber tracking in alcoholic men and women: selective relations to dissociable functions. Alcohol Clin Exp Res 34:1201–1211. [PubMed: 20477772]

Pfefferbaum A, Sullivan EV, Hedehus M, Adalsteinsson E, Lim KO, Moseley M (2000) In vivo detection and functional correlates of white matter microstructural disruption in chronic alcoholism. Alcohol Clin Exp Res 24:1214–1221. [PubMed: 10968660]

Pitel AL, Chanraud S, Rohlfing T, Pfefferbaum A, Sullivan EV (2012a) Face-name association learning and brain structural substrates in alcoholism. Alcohol Clin Exp Res 36:1171–1179. [PubMed: 22509954]

Pitel AL, Chanraud S, Sullivan EV, Pfefferbaum A (2010) Callosal microstructural abnormalities in Alzheimer's disease and alcoholism: same phenotype, different mechanisms. Psychiatry Res 184:49–56. [PubMed: 20832253]

Pitel AL, Chetelat G, Le Berre AP, Desgranges B, Eustache F, Beaunieux H (2012b) Macrostructural abnormalities in Korsakoff syndrome compared with uncomplicated alcoholism. Neurology 78:1330–1333. [PubMed: 22496200]

Porjesz B, Begleiter H, Bihari B, Kissin B (1987) The N2 component of the event-related brain potential in abstinent alcoholics. Electroencephalogr Clin Neurophysiol 66:121–131. [PubMed: 2431876]

Rulseh AM, Keller J, Tintera J, Kozisek M, Vymazal J (2013) Chasing shadows: what determines DTI metrics in gray matter regions? An in vitro and in vivo study. J Magn Reson Imaging 38:1103–1110. [PubMed: 23440865]

Schuckit MA, Gold EO, Croot K, Finn P, Polich J (1988) P300 latency after ethanol ingestion in sons of alcoholics and in controls. Biol Psychiatry 24:310–315. [PubMed: 3401524]

Schulte T, Muller-Oehring EM, Sullivan EV, Pfefferbaum A (2012) White matter fiber compromise contributes differentially to attention and emotion processing impairment in alcoholism, HIV-infection, and their comorbidity. Neuropsychologia 50:2812–2822. [PubMed: 22960416]

Shallice T (1982) Specific impairments of planning. Philos Trans R Soc Lond B Biol Sci 298:199–209. [PubMed: 6125971]

Smith JL, Mattick RP, Jamadar SD, Iredale JM (2014) Deficits in behavioural inhibition in substance abuse and addiction: a meta-analysis. Drug Alcohol Depend 145:1–33. [PubMed: 25195081]

Song SK, Yoshino J, Le TQ, Lin SJ, Sun SW, Cross AH, Armstrong RC (2005) Demyelination increases radial diffusivity in corpus callosum of mouse brain. Neuroimage 26:132–140. [PubMed: 15862213]

Squeglia LM, Jacobus J, Tapert SF (2014a) The effect of alcohol use on human adolescent brain structures and systems. Handb Clin Neurol 125:501–510. [PubMed: 25307592]

Squeglia LM, Rinker DA, Bartsch H, Castro N, Chung Y, Dale AM, Jernigan TL, Tapert SF (2014b) Brain volume reductions in adolescent heavy drinkers. Dev Cogn Neurosci 9:117–125. [PubMed: 24632141]

Steinbrink C, Vogt K, Kastrup A, Muller HP, Juengling FD, Kassubek J, Riecker A (2008) The contribution of white and gray matter differences to developmental dyslexia: insights from DTI and VBM at 3.0 T. Neuropsychologia 46:3170–3178. [PubMed: 18692514]

Sullivan EV, Deshmukh A, De Rosa E, Rosenbloom MJ, Pfefferbaum A (2005) Striatal and forebrain nuclei volumes: contribution to motor function and working memory deficits in alcoholism. Biol Psychiatry 57:768–776. [PubMed: 15820234]

Sullivan EV, Harris RA, Pfefferbaum A (2010) Alcohol's Effects on Brain and Behavior. Alcohol research & health : the journal of the National Institute on Alcohol Abuse and Alcoholism 33:127–143. [PubMed: 23579943]

Sullivan EV, Pfefferbaum A (2005) Neurocircuitry in alcoholism: a substrate of disruption and repair. Psychopharmacology (Berl) 180:583–594. [PubMed: 15834536]

Sun SW, Liang HF, Trinkaus K, Cross AH, Armstrong RC, Song SK (2006) Noninvasive detection of cuprizone induced axonal damage and demyelination in the mouse corpus callosum. Magn Reson Med 55:302–308. [PubMed: 16408263]

Tamnes CK, Walhovd KB, Engvig A, Grydeland H, Krogsrud SK, Ostby Y, Holland D, Dale AM, Fjell AM (2014) Regional hippocampal volumes and development predict learning and memory. Dev Neurosci 36:161–174. [PubMed: 24902771]

Thayer RE, Callahan TJ, Weiland BJ, Hutchison KE, Bryan AD (2013) Associations between fractional anisotropy and problematic alcohol use in juvenile justice-involved adolescents. Am J Drug Alcohol Abuse 39:365–371. [PubMed: 24200206]

Thiebaut de Schotten M, Dell'Acqua F, Ratiu P, Leslie A, Howells H, Cabanis E, Iba-Zizen MT, Plaisant O, Simmons A, Dronkers NF, Corkin S, Catani M (2015) From Phineas Gage and Monsieur Leborgne to H.M.: Revisiting Disconnection Syndromes. Cereb Cortex 25:4812–4827. [PubMed: 26271113]

Treit S, Lebel C, Baugh L, Rasmussen C, Andrew G, Beaulieu C (2013) Longitudinal MRI reveals altered trajectory of brain development during childhood and adolescence in fetal alcohol spectrum disorders. J Neurosci 33:10098–10109. [PubMed: 23761905]

Tyszka JM, Readhead C, Bearer EL, Pautler RG, Jacobs RE (2006) Statistical diffusion tensor histology reveals regional dysmyelination effects in the shiverer mouse mutant. Neuroimage 29:1058–1065. [PubMed: 16213163]

Wang J, Wai Y, Lin WY, Ng S, Wang CH, Hsieh R, Hsieh C, Chen RS, Lu CS (2010a) Microstructural changes in patients with progressive supranuclear palsy: a diffusion tensor imaging study. J Magn Reson Imaging 32:69–75. [PubMed: 20578012]

Wang Q, Xu X, Zhang M (2010b) Normal aging in the basal ganglia evaluated by eigenvalues of diffusion tensor imaging. AJNR Am J Neuroradiol 31:516–520. [PubMed: 19892817]

Yushkevich PA, Piven J, Hazlett HC, Smith RG, Ho S, Gee JC, Gerig G (2006) User-guided 3D active contour segmentation of anatomical structures: significantly improved efficiency and reliability. Neuroimage 31:1116–1128. [PubMed: 16545965]

Zahr NM, Pfefferbaum A (2017) Alcohol's Effects on the Brain: Neuroimaging Results in Humans and Animal Models. Alcohol Res 38:183–206. [PubMed: 28988573]

Zahr NM, Pfefferbaum A, Sullivan EV (2017) Perspectives on fronto-fugal circuitry from human imaging of alcohol use disorders. Neuropharmacology 122:189–200. [PubMed: 28118989]

Zhan W, Kang GA, Glass GA, Zhang Y, Shirley C, Millin R, Possin KL, Nezamzadeh M, Weiner MW, Marks WJ, Jr., Schuff N (2012) Regional alterations of brain microstructure in Parkinson's disease using diffusion tensor imaging. Mov Disord 27:90–97. [PubMed: 21850668]

Zhao DD, Zhou HY, Wu QZ, Liu J, Chen XY, He D, He XF, Han WJ, Gong QY (2012) Diffusion tensor imaging characterization of occult brain damage in relapsing neuromyelitis optica using 3.0T magnetic resonance imaging techniques. Neuroimage 59:3173–3177. [PubMed: 22108642]

Zorlu N, Karavul Ucman T, Gelal F, Colak Kalayci C, Polat S, Saricicek A, Kurtgoz Zorlu P, Gulseren S (2014) Abnormal white matter integrity in long-term abstinent alcohol dependent patients. Psychiatry Res 224:42–48. [PubMed: 25104315]

Zou X, Durazzo TC, Meyerhoff DJ (2018) Regional Brain Volume Changes in Alcohol-Dependent Individuals During Short-Term and Long-Term Abstinence. Alcohol Clin Exp Res 42:1062–1072. [PubMed: 29672876]

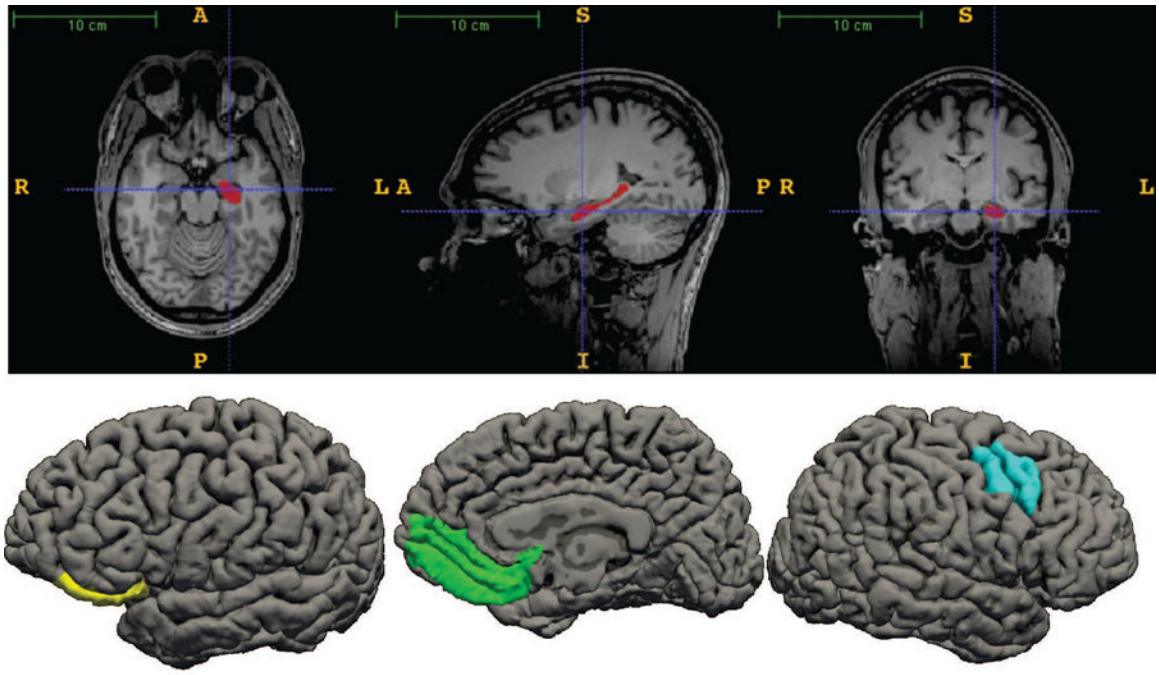

Figure 1:

(1a) Axial, sagittal, and coronal sections through the left hippocampus of a test participant measured using the automatic segmentation method, and (1b) Cortical volumes found to be significantly different between groups (left parsorbitalis, right medial orbitofrontal, and right caudal middle frontal cortices).

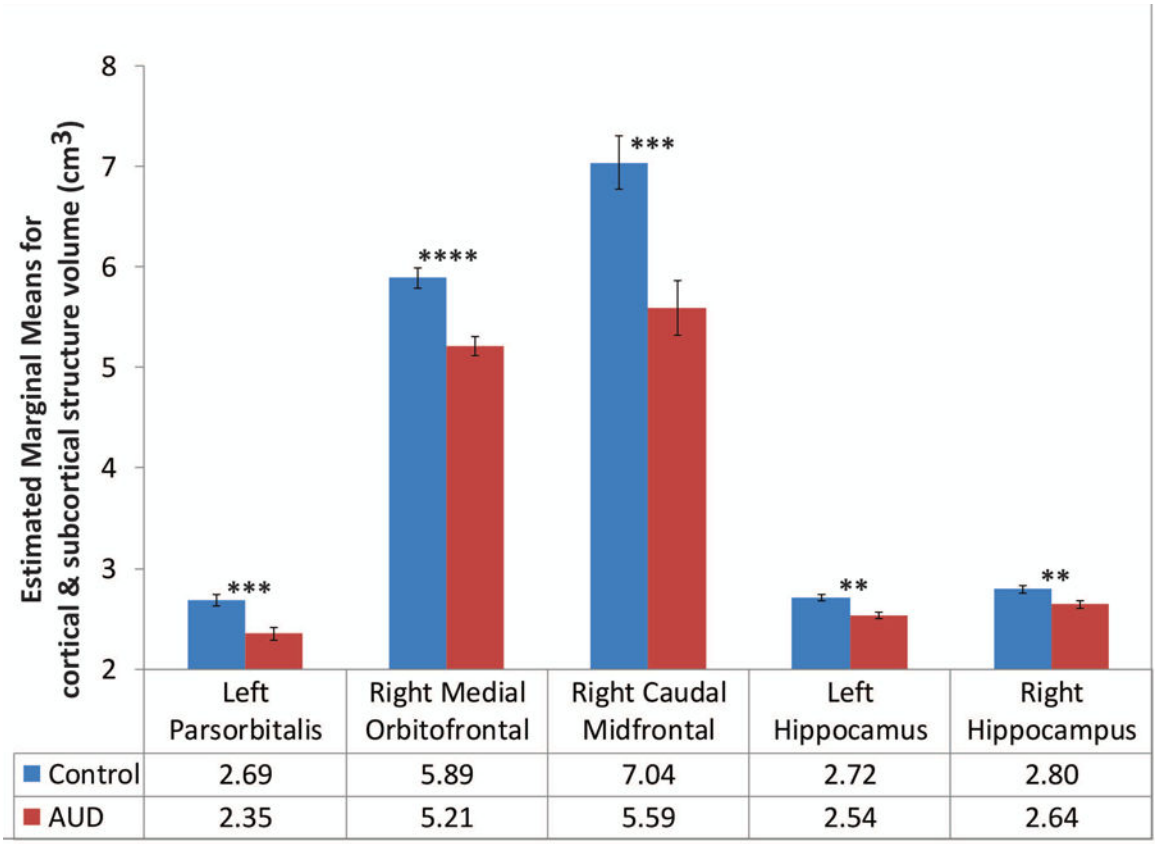

	Left Parsorbitalis	Right Medial Orbitofrontal	Right Caudal Midfrontal	Left Hippocampus	Right Hippocampus
Control	2.69	5.89	7.04	2.72	2.80
AUD	2.35	5.21	5.59	2.54	2.64

Figure 2:

Estimated marginal means (EMM; color bars) and standard error (SE; error bars) of cortical and subcortical volumes of AUD (red) and control (blue) groups.**** $p<0.0002$, *** $p<0.002$, ** $p<0.008$

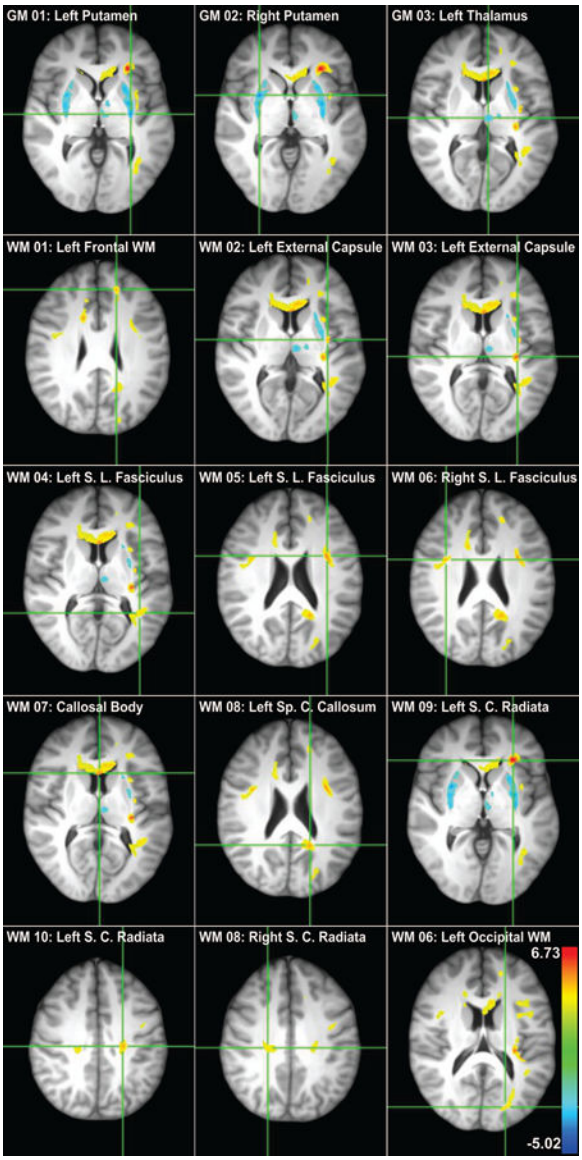

Figure 3:

Regions showing group differences in FA. Cool colors (blue) indicate higher FA in AUD participants; warm colors (red and yellow) indicate higher FA in controls.

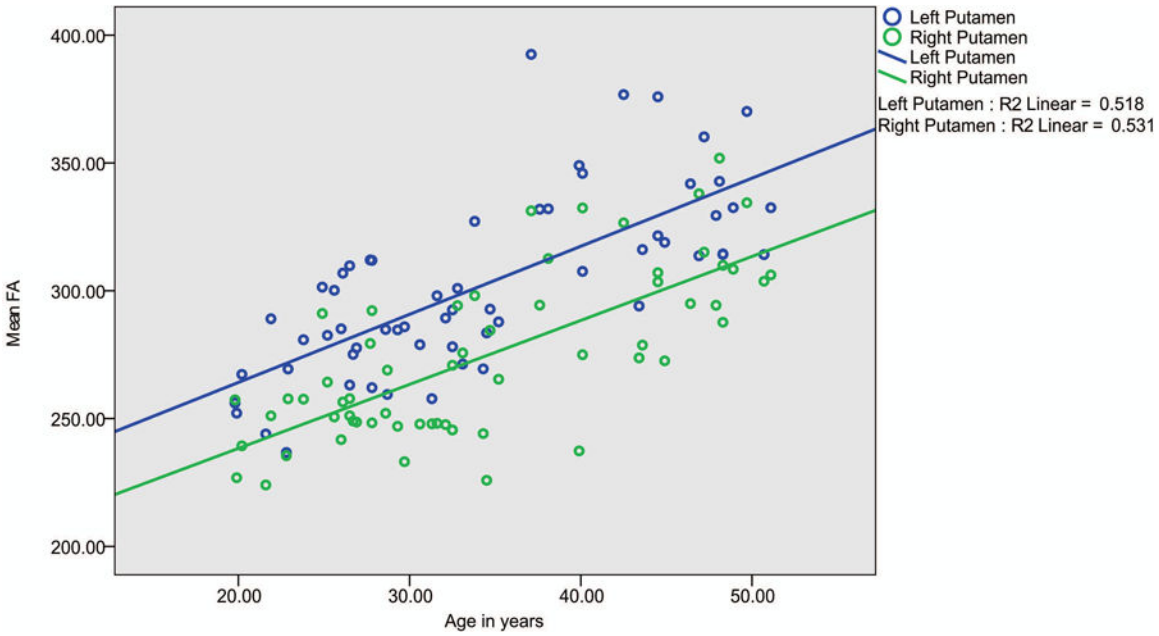

Figure 4:

Scatter plot and fit line showing high positive correlation of Mean FA values in bilateral putamen with increasing age.

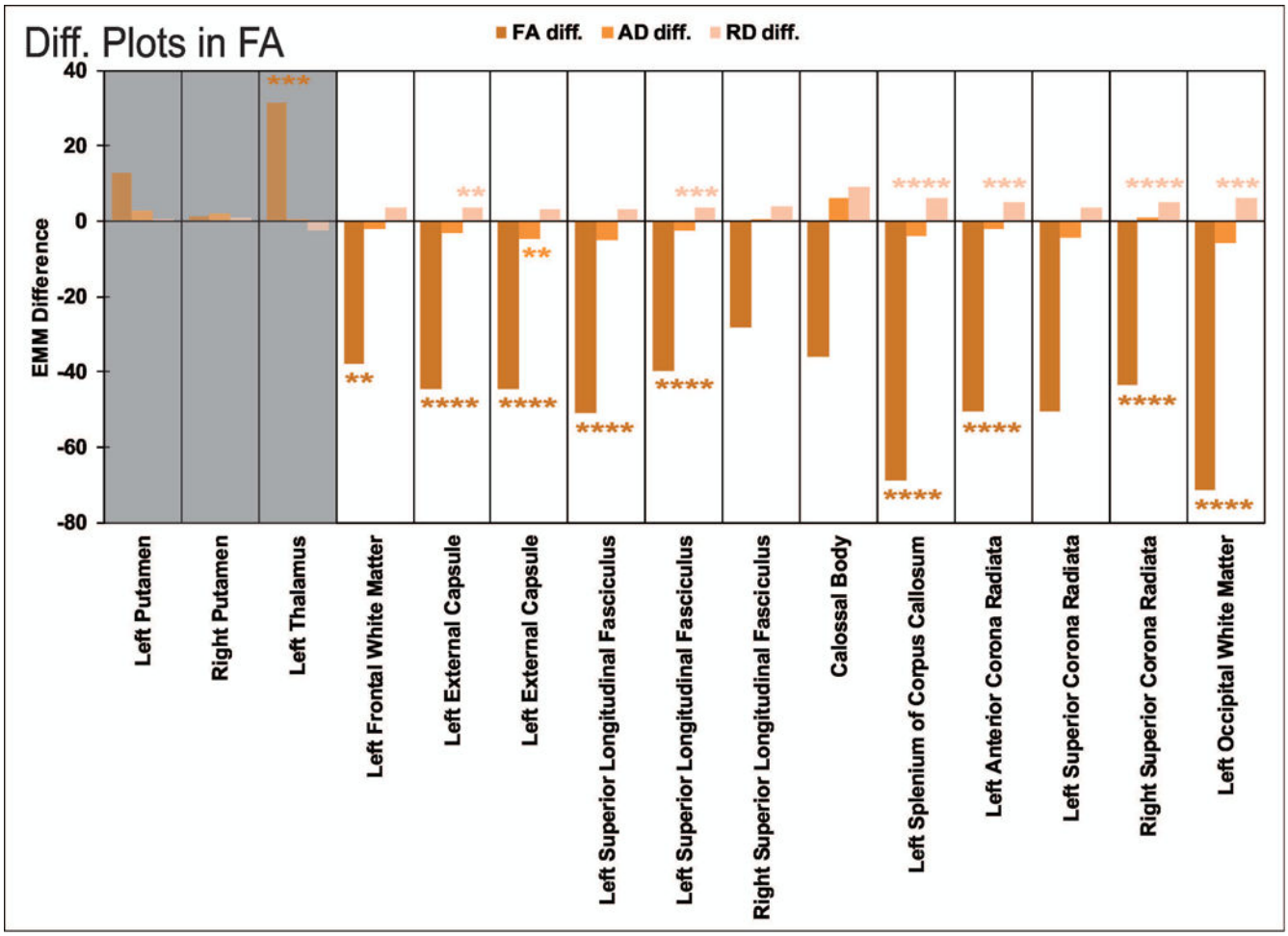

Figure 5:

Direction of differences in estimated marginal means (EMM) for the 15 FA clusters and their average AD, and RD values. Clusters from GM regions are shown in gray shaded background and WM regions are shown in white background.

Table 1:

Alcohol and substance use profile of AUD and control subjects.

	AUD			Control		
	N[*]	Mean	SD	*N*[*]	Mean	SD
Age of onset (regular alcohol use[≠])	30	15.77	2.58	12	20.50	3.80
Alcohol: Drinks/day (heavy alcohol use period)	30	12	10.02	12	3	1.93
Alcohol: Days/month (heavy alcohol use period)	30	20	9.01	12	3	3.64
Alcohol: Drinks (last 6 months)	30	3	6.61	18	3	1.98
Alcohol: Days (last 6 months)	30	4	8.02	18	3	3.62
Length of Abstinence (in days)	30	672.93	844.94	18	57	149.76
Tobacco: Times/day (last 6 months)	20	10	5.80	6	2	1.63
Tobacco: Days/month (last 6 months)	20	28	4.83	6	14	13.82
Marijuana: Times in last 6 months	10	99	91.38	4	19	27.61

AUD = Alcohol Use Disorder, N = Number of subjects, SD = Standard deviation.

[*]Note that N's refer to those who meet criteria for the alcohol and substance use variables; all subjects were assessed and were omitted from the table if they did not meet these criteria.

[≠]One drink per month for six months or more

Table 2:

15 FA clusters and average AD and RD values in these clusters, their types, sizes, MNI coordinates, locations, F values, significances, and direction of differences between AUD and controls.

CT	Size (mm^3)	MNI	Location	F (FA)	*p* val.	Direction	F (AD)	*p* val.	Direction	F (RD)	*p* val.	Direction
GM01	2643	-29, −13, 1	LPut	1.83	0.182	NS	5.68	0.021	NS	0.277	0.601	NS
GM02	2097	31, 5, −1	RPut	0.02	0.886	NS	3.24	0.077	NS	1.48	0.228	NS
GM03	688	-4, −16, 8	LTha	12.22	0.001	**A>C**	0.12	0.732	NS	5.39	0.024	NS
WM01	764	-16, 39, 28	LFroWM	7.87	0.007	**A<C**	1.65	0.204	NS	5.64	0.021	NS
WM02	657	-34, −8, 8	LExCap	18.73	0.000	**A<C**	5.10	0.028	NS	9.81	0.003	**A>C**
WM03	711	-31, −24, 10	LExCap	19.91	0.000	**A<C**	8.26	0.006	**A<C**	5.59	0.022	NS
WM04	1529	-38, −49, 10	LSupLF	14.58	0.000	**A<C**	7.36	0.009	NS	4.37	0.041	NS
WM05	1915	-33, 5, 23	LSupLF	19.91	0.000	**A<C**	2.35	0.131	NS	11.59	0.001	**A>C**
WM06	782	36, 2, 25	RSupLF	5.63	0.021	NS	0.03	0.874	NS	7.47	0.008	NS
WM07	4816	0, 18, 10	CalB	7.61	0.008	NS	1.89	0.175	NS	3.21	0.079	NS
WM08	783	-17, −50, 24	LSpCCal	22.57	0.000	**A<C**	2.65	0.109	NS	19.49	0.000	**A>C**
WM09	1832	-27, 30, 0	LAntCR	23.76	0.000	**A<C**	2.40	0.127	NS	11.38	0.001	**A>C**
WM10	575	-22, −23, 40	LSupCR	6.36	0.015	NS	4.08	0.048	NS	4.58	0.037	NS
WM11	1029	23, −25, 37	RSupCR	19.03	0.000	**A<C**	0.34	0.564	NS	17.46	0.000	**A>C**
WM12	782	-19, −81, 16	LOccWM	23.06	0.000	**A<C**	6.74	0.012	NS	12.04	0.001	**A>C**

Ant = Anterior, CalB = Callosal Body, CT = Cluster Type, CR = Corona Radiata, ExCap = External Capsule, Fro = Frontal, GM = Gray Matter, L = Left, LF = Longitudinal Fasciculus, MNI = Montreal Neurological Institute Coordinates, NS = Not significant, Occ = Occipital, Put = Putamen, p val. = p value R = Right, SE = Standard Error, SPCCal = Splenium of Corpus Callosum, Sup = Superior, Tha = Thalamus, WM = White Matter.

Table 3:

Difference estimates between controls (ctl) and alcoholics (alc), SE, t-test, and *p* values of significant neuropsychological measures.

Variable		Difference (ctl – alc)	SE	t value	*p*value
TOLT	**EM_3B**	-0.68	0.32	-2.12	0.034 *
	TC_F	1.67	0.67	2.50	0.013 *
VST	**Span_F**	1.77	0.55	3.20	0.001 **
	Span_B	1.18	0.54	2.19	0.029 *

** $p<0.01$

* $p<0.05$, SE = Standard Error, EM_3B = Excess moves-3 pegs/beads, Span_F = Forward span, Span_B = Backward span, TC_F = Total correct forward span.

Table 4:

Canonical solution for volumetric measures predicting neuropsychological task performances for dimension 1.

Variable set	Variable	Dimension 1		
		R_c	R_s	R_s^2 (%)
Set 1	**LParsOrbV**	0.59	**0.48**	**23.04**
	RMeOFV	0.17	**0.33**	**10.89**
	RCMiFV	0.38	**0.42**	**17.64**
	LHV	0.54	**0.36**	**12.96**
	RHV	-0.64	0.19	3.61
Set 2	**EM_3B**	0.06	**-0.39**	**15.21**
	Span_F	-0.32	**0.87**	**75.69**
	TC_F	1.29	**0.99**	**98.01**
	Span_B	0.12	**0.64**	**40.96**

EM_3B = Excess moves-3 pegs/beads puzzle-type, LHV = Left hippocampal volume, LParsOrbV = Left parsorbitalis volume, R_C = Standardized canonical dimension coefficient, RCMiFV = Right caudal middle frontal volume, RHV = Right hippocampal volume, RMeOFV = Right medial orbitofrontal volume, R_S = Structure coefficient, R_S^2 = Squared structure coefficient, Span_B = Backward span, Span_F = Forward span, TC_F = Total correct trial-count for forward memory span.

Table 5:

Canonical solution for FA values predicting neuropsychological task performance for dimension 1.

Variable set	Variable	Dimension 1		
		R_c	R_s	R_s^2 (%)
Set 1	**GM03**	-0.26	**-0.35**	**12.25**
	WM01	0.31	**0.44**	**19.36**
	WM02	-0.97	0.17	2.89
	WM03	0.31	0.28	7.84
	WM04	0.09	0.31	9.61
	WM05	0.05	**0.55**	**30.25**
	WM08	0.11	**0.36**	**12.96**
	WM09	-0.01	**0.34**	**11.56**
	WM11	-0.31	0.29	8.41
	WM12	0.10	0.28	7.84
Set 2	**EM_3B**	-0.09	**-0.41**	**16.81**
	Span_F	-0.33	**0.87**	**75.69**
	TC_F	1.46	**0.97**	**94.09**
	Span_B	-0.29	**0.41**	**16.81**

EM_3B = Excess moves-3 pegs/beads puzzle-type, GM = Gray matter, R_C = Standardized canonical dimension coefficient, R_C^2 = Squared Standardized canonical dimension coefficient, R_S = Structure coefficient, R_S^2 = Squared structured coefficient, Span_B = Backward span, Span_F = Forward span, TC_F = Total correct trial-count for forward memory span, WM = White matter.